IOP Conf. Series: Materials Science and Engineering **758** (2020) 012048 doi:10.1088/1757-899X/758/1/012048

A 3-D Analysis on the Loading Behaviours of an Under-reamed Anchor in Cohesion-less Soils

Shih-Tsung Hsu[1], Xiang-Yang Chen[2]and Yi-Fan Wang[3]

1Professor and Chairman, Department of Construction Engineering, Chaoyang University of Technology, Taichung, TW
2 Lecturer, School of Civil Engineering and Architecture, Nantong Vocational University, Nantong, CN
3 Master student, Department of Construction Engineering, Chaoyang University of Technology, Taichung, TW
E-mail:sthsu@cyut.edu.tw

Abstract. This study adopts a constitutive model for sand and a 3-D numerical software, named "FLAC^{3D}" to examine the anchorage behaviours of an under-reamed anchor in sandy soil. A series of pull-out test on model anchors is performed to confirm the results obtained numerical analyses. Test results reveal that the load-movement curves computed numerically are get close to those estimated experimentally. For under-reamed anchors with dimensions of D=0.075m, L/D=4.5, and installed in sandy soil of D_r=70% (D_r: relative density, D: diameter of anchor, L/D: fixed end/diameter ratio), the shape of load-movement relationship on a deep anchor differs from that of a shallow anchor, especially the shape of end resistance-movement curve. However, the friction force, end resistance and total load do not attain peak values at same anchor movement. The end resistance of a shallow anchor displays obviously peak value. However, the peak value the end resistant cannot treasured from a deep anchor. The friction load presents peak and residual values. The mainly pull-out load of a shallow anchor is donated by the friction load, meanwhile the end bearing governs the pull-out load of a deep anchor; overburden depth of 12D is the shallow/deep anchor demarcation. According to the definition of end bearing coefficient, it is categorised to a deep anchor as the overburden surpasses 12D, it is a shallow anchor if the overburden is smaller than 7.5D, and as the overburden equal to 7.5D~12D, the anchor can be classified as a transit anchor.

1. Introduction

Foundations of diverse structures, such as submerged pipelines and transmission towers, are frequently applied huge lift forces. The application of ground anchors as part of a foundation system looks to be a feasible choice for preserving the stability and increasing a vertical uplift capacity of the structure. Additionally, vertical anchors are commonly applied to offset eccentric forces that load on foundation mats, to fix basements against uplift pressure resulting from groundwater, or to resist seismic force.

The top stratum of the Taipei Basin comprises the Sung-Shan formation, depending on the local geological characteristics, the thickness of which ranges from 30 to 60 m. Nearly all of the fixed anchor lengths of the anchors installed in the Taipei Basin are in the Sung-Shan formation, which contents of alternating layers of clay and sand. The fixed lengths are naturally located in sandy layers. In some places, however, the thickness of the sand that provides shear strength is restricted. As a result, an anchor with both of high anchorage load and short fixed length is necessary in this scenario.

To achieve both of high anchorage load and short fixed length in an anchor, Hsu and Liao [1] recommended the under-reamed anchor, which has an equal diameter in its fixed length. As displayed in Figure 1(a) is the under-reamed anchor, the fixed anchor is formed by the enlarged blade system. Initially, the device with four blades remains closed. When the drilling rod drills to the pre-set depth, all four blades are opened and turn around concurrently to expand the fixed length. The diameter can be determined by the length and rotating rate of the blades. After enlargement, the drilling rod is substituted by the strand system coupled to the swivel. A grout with the water/cement ratio of W/C=0.45~0.55 is then pressurized at 1 MPa to produce the under-reamed length. In accordance with the mechanism of load transfer within the fixed length, the anchor is categorized as a kind of compression anchor.

Studies on anchorage behavior of anchors are various, and can be categorized into several fields, such as field tests [2], model tests [3], limit analyses [4] and numerical analyses [5]. For field tests, most tested anchors are not stressed until failure; thus, their ultimate loads cannot be estimated accurately. The limit analysis cannot realistically examine the pre- and post-peaks of soil behavior. Regarding numerical analyses, these seldom use a fair stress-strain relationship for soil that includes strain softening to research the anchorage behavior, a complete load-movement curve of an anchor cannot be calculated precisely.

Therefore, a precisely numerical model and an analyzed method are demeaned to investigate the behavior of ground anchor, and the loading behaviors of under-reamed anchors are necessary to be researched further.

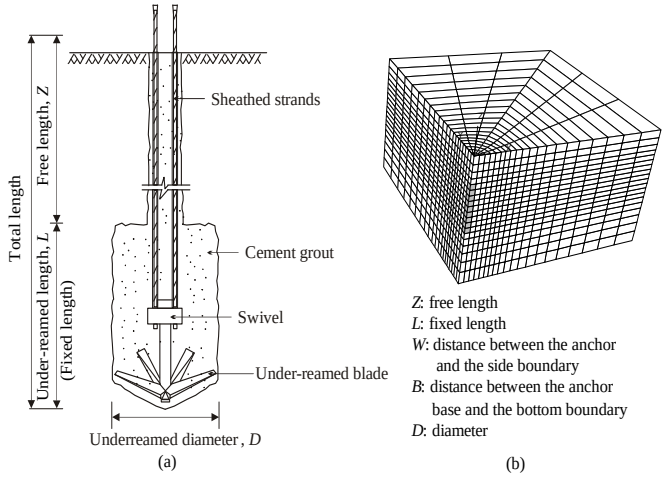

Figure 1. Illustration of an under-reamed anchor and represnetative meshes for numerical analysis (Z/D=2.5、L/D=4.5).

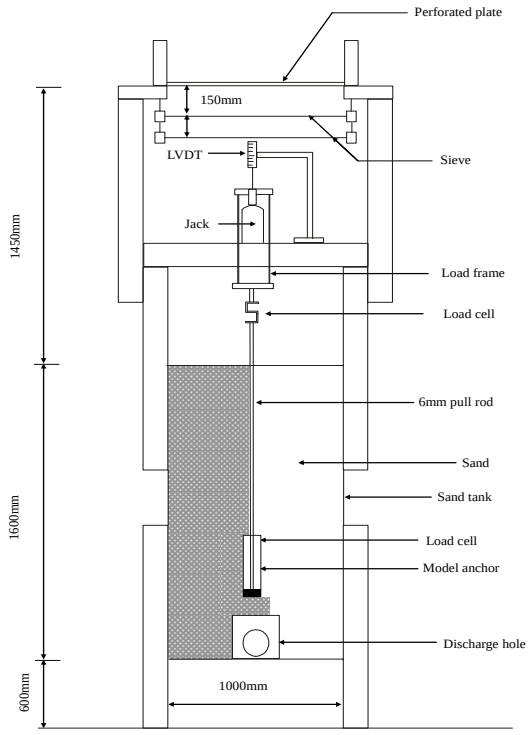

Figure 2. The experimental model anchor test's setups.

2. Numerical Model of Sand and Analytical Method

Hsu and Liao[1] recommanded a numerical model that consists both the strain hardening/softening and volumetric dilatancy, called *SHASOVOD* model. The model had been adopted with the software FLAC^{2D} to study the anchorage behaviours of several types of anchors in sandy soil. The results

revealed that the numerical results were consistent with those results obtained in-situ. Therefore, this work applies above model and the commerical software FLAC^{3D} to research the anchorage behavior of an under-reamed anchor in sandy soil.

The sandy specimen is taken from Yi-lan, it is classified as the *SP*-type soil, its specific gravity G_s of 2.69, which with a minimum dry unit weight of 13.70 kN/m^3, and a maximum dry unit weight of 17.34 kN/m^3.

The numerical model is related to the non-associated flow rule of plasticity theory. The yield function *f* can be expressed as

$$f = \sigma_1 - \sigma_3 \frac{1+\sin\phi^*}{1-\sin\phi^*} \tag{1}$$

where ϕ^* is the mobilized friction angle, which is related to accumulative plastic strain ε^p; and σ_3 denotes the minor principal stress, σ_1 represents the major principal stress. The plastic potential function g is

$$g = \sigma_1 - \sigma_3 \frac{1+\sin\psi^*}{1-\sin\psi^*} \tag{2}$$

where ψ^* resprents the mobilized dilatancy angle, and related to accumulative plastic strain ε^p. To illustrate the reliability of the numerical model, the stress-strain relations of sand with a relative density of 70%, calculated using the proposed model, are used to compare with those evaluated from triaxial test. As depicted in Figure 3, the triaxial test results get perfectly close to the results from numerically calculated results. Hsu and Liao [6] elucidated the relevant details of the model.

The assumptions for numerical analyses are listed as followings

- The fixed anchor (under-reamed length) is elastic and homogenous.
- The load is uniformly applied to the bottom of the anchor, because the under-reamed anchor is a compression anchor; and
- To reduce calculated consumption, one-quarter symmetric meshes are used for the under-reamed anchor.

Figure 1(b) illustrates the representative numerical meshes and details adopted to depict an anchor.

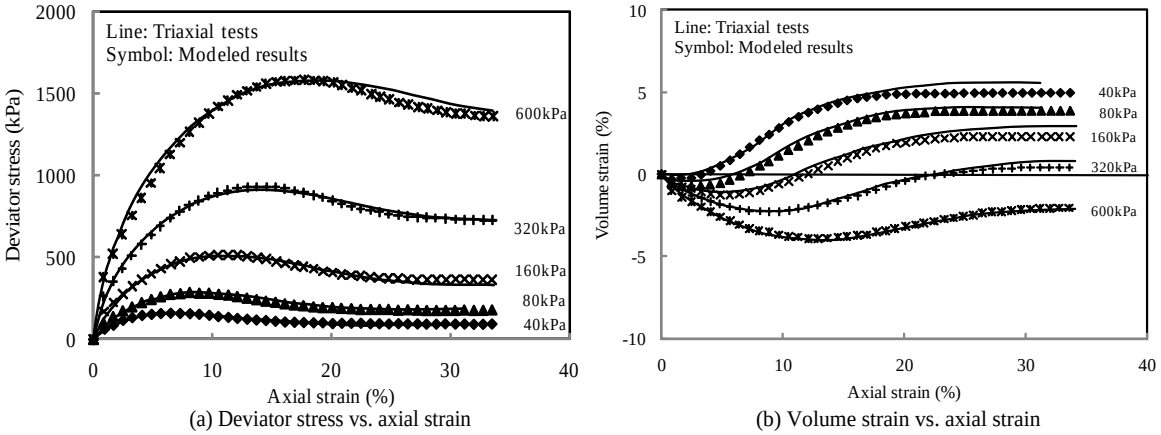

(a) Deviator stress vs. axial strain (b) Volume strain vs. axial strain

Figure 3. Tested and calculated deviator stress-axial strain-volume strain curves (D_r=70%).

3. Verifications of Numerical results

3.1. Experimental Model Tests

In engineering practice, the length/diameter ratios, L/D for under-reamed anchors can be ranged from 2.5~5.0. However, an under-reamed anchor with an L/D ratio of 4.5 for generating both shaft friction and end bearing is adopted for the model tests and numerical analyses in this paper.

The model anchor employed for the experimental test is made of aluminum tube, the diameter is 75 mm, length is 338 mm, and L/D is 4.5. The surface of the tube is corrugated in a pitch of 1.6 mm.

As shown in Figure 2, the anchor is installed in the center of a container. Sand particles fall freely into the container from a punctured plate with holes' diameter of 8 mm and throughout two sieves of opening dimension of 3 mm, the processes can produce a relative density of around 70%. When the sand surface reached the top of the container, the sand raining is stopped. Finally, the model anchor is pulled vertically during the whole pull-out processes at rate of 1mm/min.

3.2. Verifications

Hsu et al. [6] suggested that an under-reamed anchor placed in sandy soil of D_r=70% is classified as a shallow anchor, when overburden depth Z smaller than 8D. Else, the anchor is categorized as a deep anchor.

Figure 4 presents the experimental and numerical load-movement relationships of under-reamed anchors with overburden depth ratios of Z/D=2.5 and 10. Figure 4 reveals that the numerically calculated load-displacement curves are consistent with those measured by laboratory tests. Therefore, this study uses the numerical method to investigate the behaviors under-reamed anchor with various overburden depths in sand.

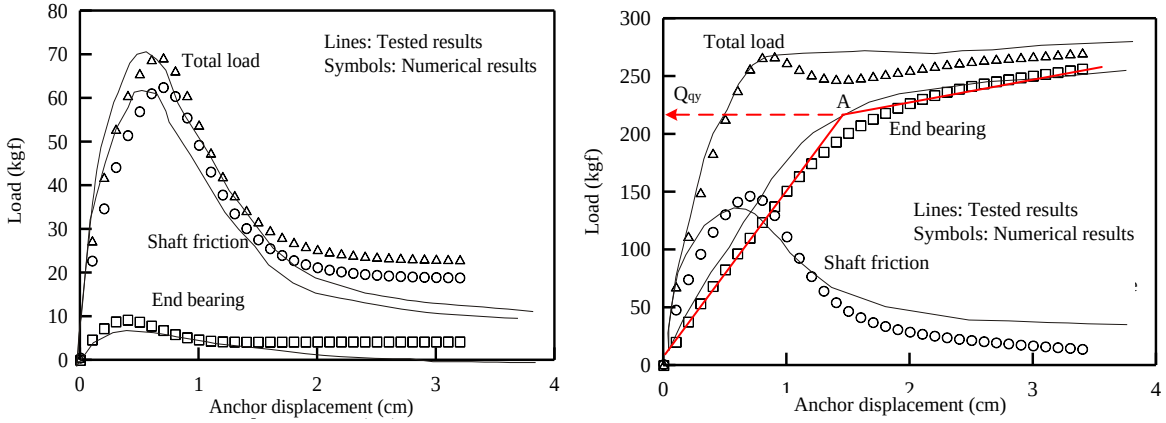

Figure 4. Numerical and experimental load-displacement (anchor movement) behaviours of two under-reamed anchors with Z/D=2.5 and Z/D=10.

4. Discussion on the experimental and numerical results

4.1. Load-displacement (anchor movement) relationships of the anchor

Figure 4 depicts the load-movement of anchor with Z/D=2.5 and 10. Figure 4(a) demostrates the total load and friction force raise with the anchor movement until the peaks take place; after that, decline obviously from peak to residual values. The end resistant exhibits a pre-peak and post-peak as well, indicating that the anchor is a typical shallow anchor of Z/D=2.5.

The friction force similarly behaves the phenomenon of pre-peak and post-peak for a deep anchor of Z/D=10 (Figure 4(b)). The end resistance of a deep anchor increases with anchor movement constantly without a peak. As a result, the total load originally declines and then rises when the anchor movement increases in the post-peak stage. For simplicity of assessment with the ultimate load of the anchors, this research defines the first peak load as the anchorage capacity for a deep anchor.

In brief, the ultimate anchor load is not the summation of peak friction load and peak end resistance (yield end bearing), because the peak total load, peak shaft friction and peak (yield) end bearing occurs

in different anchor movements. Additionally, a greater overburden depth ratio Z/D indicates a greater corresponding anchor movement of the ultimate end bearing; and when the anchors are installed in the relative densities of 70%, with overburdens that exceeds 7.5D, the end bearings increase without peaks. Because the anchor's overburden exceeds the critical overburden depth H, no peak can be found on end bearing [6]. To decide the amount of the end resistance depicted formerly, an artificial recommendation by Trautmann and Kulhawy[7] is adopted. Figure 4(b) is the numerical end resistance-movement relations, Point A is obtained from the intersection of the initial tangent line and the latter half section of an end resistance-movement curve, and the ordinate that corresponded to Point A is the yielding end resistance Q_{qy} of an under-reamed anchor that had an end bearing without a peak.

4.2. Differentiating a shallow anchor from a deep anchor by coefficient of end bearing

This study applied the coefficient of end bearing N_q to classify an anchor as a shallow anchor or deep ancho. For anchors installed in cohesion-less soil, the coefficient of end bearing N_q can be expressed as

$$N_q = \frac{Q_q}{\gamma\ Z\ A_q} \tag{3}$$

where Q_q denotes the end bearing of an anchor, γ is the unit weight of the silty sand, Z represents the overburden (free length) of an anchor, and $A_q$is the cross-area of the fixed end.

Based on Equation (3), the relationship between the coefficient of an end bearing and the overburden/diameter ratio is plotted and is shown in Figure 5. The curve depicted in Figure 5 appears to increase and is initially upwardly concave. Consequently, the curve increases and becomes downwardly concave. The point of inflection in respect to the overburden is labelled as the critical overburden depth of shallow anchor *H*, as suggested by Vermeer and Sutjiadi [8]. The *H*is 7.5*D*. When the overburden depth is shallower than the critical overburden depth *H*, an obvious peak is found on end bearing-displacement curves, and the yielding soil around the under-reamed length develops to the ground surface, the anchor is a shallow anchor.

When the overburden depth exceeds 12*D* for anchors in sand, the coefficient N_q decreases with *Z/D*, the maximum in the curve corresponding to the overburden is the critical depth of transited anchor H_1. When the overburden of an anchor exceeded *H* but was smaller than H_1, the anchor belonged to a transited anchor. The anchor's end bearing-displacement does not have a peak, but the yielding soil around the anchor developed to the ground surface. However, when the overburden depth of an anchor exceeds H_1, the anchor is categorized as a deep anchor, and the end bearing-displacement curve does not behave a peak, the yielding soil around the under-reamed length does not develop to the ground surface.

Three types of anchors are found based on the relationship between the coefficient of end bearing N_q and overburden *Z*: shallow, transited, and deep anchors. These have behaviors that are similar to those of general shear failure, local shear failure, and punching shear failure in shallow foundations.

4.3. Dividing an end-bearing anchor from a frictional anchor

Anchorage capacity comprises the end bearing and friction load. Therefore, it is worthwhile to differentiate whether an anchor is an end-bearing or friction type. Research results indicated that the proportions of end bearing and friction load changed when the overburden and fixed length/diameter ratio were changed. When the fixed length remains unchanged, the proportion of friction decreases with the increase in the overburden/diameter ratio Z/D, the proportions of the end bearing and friction remains approximately constant until the Z/D exceeds 16. Figure 6 shows the percentages of the end bearing and friction load that dominates the anchorage capacity versus the Z/D for an anchor with a L/D of 4.5. Figure 6 demonstrates that when the Z/D is less than 10, the anchor is categorized as an end-bearing type; otherwise, it is a friction anchor.

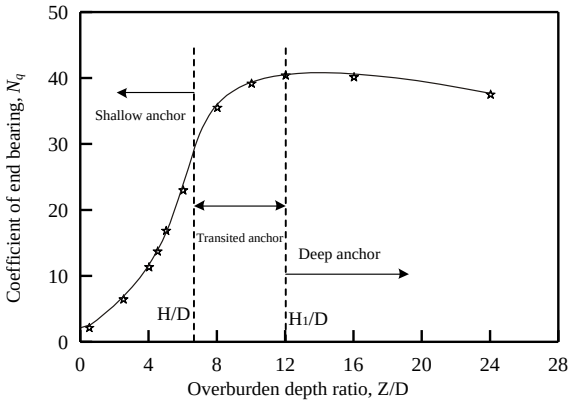

Figure 5. Relationship between coefficient ofend bearing and overburden depth/diameter ratio.

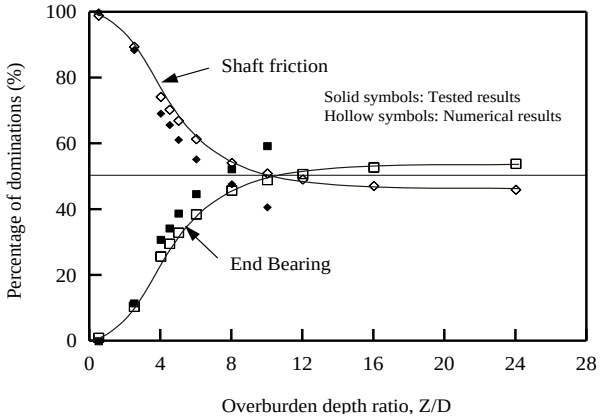

Figure 6. Percentages of end bearing and friction that dominate the loading capacity when peak load is applied.

5. Conclusion

This study adopted both the laboratory model test and numerical investigation to examine behaviours of under-reamed anchors in dense sand with a verity of overburden/diameter ratio Z/D. The results pilot the conclusion as following

- Research results demonstrated that the load-movement relationships evaluated numerically are in an agreement with those obtained experimentally. Hence, the numerical model together with FLAC^{3D} software could evaluated the behaviour of under-reamed anchor perfectly.
- The shapes of load-movement relationships on deep anchors were different from those of shallow anchors, especially the shapes of end resistance-movement curves.
- The frictional force dominated the ultimate load of a shallow anchor; meanwhile the end resistance is the main part of total load for a deep anchor. The demarcation overburden depth was 12D.
- According to the categorization of end bearing coefficient, if an overburden less than 7.5D, it was a shallow anchor; when an overburden exceeded 12D, it was classified to a deep anchor; and as an overburden depth was between 7.5D~12D, the anchor belonged to a transit anchor.

6. Reference

[1] Hsu S T and Liao H J 1998 Uplift behavior of cylindrical anchors in sand *Canadian Geotechnical Journal* vol 35 no1 p 70-80

[2] Liao H J Ou C D and Hsu S T 1996 Anchorage behavior of shaft anchors in alluvial soil *Journal of Geotechnical Engineering Division* (ASCE) vol 122 no 77 p 526-533.

[3] Hanna T H Sparks R Yilmaz M 1972 Anchor behavior in sand J*ournal of the Soil Mechanics and Foundation Division* (ASCE) vol 98 no 11 p 1187-1208

[4] Ganesh R Khuntia S and Sahoo J P 2018 Seismic uplift capacity of shallow strip anchors: A new pseudo-dynamic upper bound limit analysis *Soil Dynamics and Earthquake Engineering* vol 109 p 69~75

[5] Wang D Hu Y Randolph M F 2010 Three-dimensional large deformation finite-element analysis of plate anchors in uniform clay *Journal of Geotechnical and Geoenvironmental Engineering*, (ASCE) vol 136 no 2 p 355–365

[6] Hsu S T Wang C C Wu S Tung H C 2016 Computer simulation on the uplift behaviors of arrayed underreamed anchor groups in sand *Systems and Informatics* (IEEE) p 534-539

[7] Trautmann C H and Kulhawy F H 1988 Uplift Load-Displacement Behavior of Spread Foundations *Journal of Geotechnical Engineering* vol 114 no 2 p 168-184